Analytical Methods

Accepted Manuscript

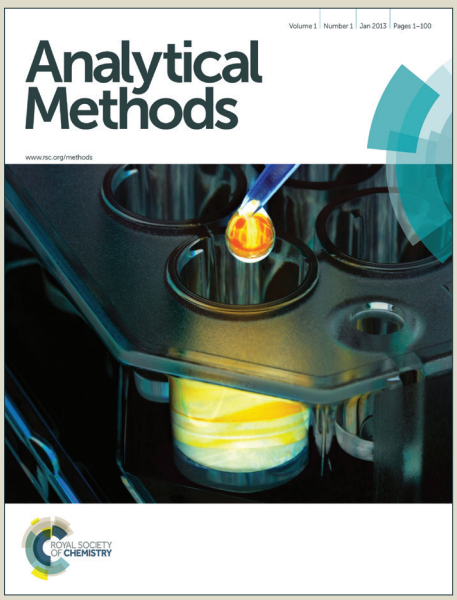

ROYAL SOCIETY OF CHEMISTRY

www.rsc.org/methods

Analytical Methods

ARTICLE

In situ simultaneous investigation of the transport of phenanthrene and fluoranthene adsorbed onto the root surfaces to tissues of mangrove seedlings †

Received 00th January 20xx,
Accepted 00th January 20xx

DOI: 10.1039/x0xx00000x

www.rsc.org/

R. L. Li,[a] H. D. Tan,[a] Y. X. Zhu,[b] and Y. Zhang*[a, c]

A novel method for the simultaneous *in situ* determination of phenanthrene (Phen) and fluoranthene (Fla) adsorbed onto mangrove root surfaces was established using laser-induced time-resolved nanosecond-fluorescence spectroscopy combined with a first-order derivative fluorometry method (D-LITRF). The linear dynamic range, detection limit and recoveries of D-LITRF and laser induced time-resolved nanosecond fluorescence spectroscopy (LITRF) were of the same order. Using the established method, the transport of Phen and Fla from the mangrove root surface to tissues was simultaneously investigated *in situ*. The transportation coefficients of the Phen and Fla adsorbed onto the root surface showed a good linear relationship with the content of root lipids, while the inhibition rates showed no significant correlation with the content of root lipids ($p > 0.05$). Further studies showed that the interaction between Fla and Phen decreased the transport kinetics, especially the slow and very slow transport kinetics. In addition, the coefficients and inhibition rates of the transport of Phen and Fla to *Kandelia obovata* (*Ko*) root tissues were evaluated at different temperatures. The results acquired by these *in situ* methods provide new information about how two PAHs components are transported from the mangrove root surface to the tissues.

Introduction

Polycyclic aromatic hydrocarbons (PAHs) are widely distributed persistent organic pollutants.[1,2] They have been of particular interest due to their carcinogenicity, mutagenicity and toxicity to biota. The US EPA defined 16 PAHs as priority pollutants.[3,4] Plants grown in PAHs-contaminated soil and sediment become contaminated mainly due to the accumulation of contaminants in the root followed by their translocation. Thus, an improved understanding of the root uptake process and its mechanisms is essential to assess plant contamination and subsequent human exposure through the food chain.[5-8]

There have been many studies focused on the processes and mechanisms of root uptake of PAHs, especially by terrestrial plants, such as the sunflower (*Helianthus annuus* L.), maize (*Zea mays* L.), tall fescue (*Festuca arundinacea* Schreb.) and so on.[9,10] However, as mangrove plants have some special features, the uptake of PAHs by mangrove roots should be specifically investigated. On one hand, mangrove sediment, a habitat of the mangrove plant, acts as an important 'sink' of PAHs in mangrove ecosystems and serves as a physical and biogeochemical barrier to PAHs along the coastline of tropical and subtropical regions. In the mangrove swamps of the Jiulong River Estuary, Fujian, China, the total PAHs can also range from 280 to 1074 ng/g on a dry weight basis. On the other hand, the root morphology and composition of the tissues of the mangrove plant are significantly different from those of terrestrial plants. [11-13]

PAHs often exist as a mixture in the environment. As nearly all PAHs have a similar physicochemical characterization, such as their hydrophobicity, their highly conjugated system and their lipophilic property, co-existing PAHs affect each other during the root uptake process.[14] Moreover, many reports have shown that the uptake of PAHs by the mangrove root includes two stages: the PAHs in the mangrove sediment are desorbed from overlying and pore water and then diffusion occurs and only part of the PAHs enter into the root tissues. The transport of PAHs from the mangrove plant root surfaces to the tissues is important in the second stage of the root uptake process.[15,16] Therefore, an investigation of the transport of two- or multi-component PAHs from the surface to the tissues is critically important to improve our understanding about the process and mechanisms of PAHs root uptake.

However, until now, there exists no appropriate *in situ* analytical method that made it impossible to investigate two or multi-component PAHs adsorbed onto mangrove root surface transport to tissues. The traditional methods for the analysis of PAHs in roots include extraction, fractionation and PAHs analysis by GC, LC, and HPLC. These traditional methods are highly sensitive, selective and accurate for the determination of two- or multi-component PAHs in environmental samples.[17,18] However, these methods cannot be used to investigate the original form of the PAHs adsorbed onto the root surface or that enter into the root tissues because these methods destroy the original form of the PAHs in the root. Similar, to the traditional method described

[a] State Key Laboratory of Marine Environmental Science (Xiamen University) Xiamen 361005, China.
[b] Department of Chemistry, College of Chemistry and Chemical Engineering, Xiamen University, Xiamen 361005, China.
[c] Zhangzhou Institute of Technology, Zhangzhou, 363000, China.
†Electronic Supplementary Information (ESI) available. See DOI: 10.1039/x0xx00000x

above, surface-enhanced Raman scattering (SERS) also destroys the original form of the PAHs in an environmental sample of either the load or sorption to the substrate of PAHs before determination.[19] In addition, some other methods for the determination of PAHs, such as the Fourier transform infrared (FTIR) and UV-vis methods, that have no pre-treatment procedure can only qualitative analyse the PAHs due to the limitations of the instruments.[20]

As PAHs have relatively high quantum yield, solid surface fluorescence (SSF) method and laser induced fluorescence method (LIF) that has been established realize *in situ* quantitative determination of single PAHs adsorbed onto mangrove leaf surfaces. [21-23] Unfortunately, the SSF and LIF method did not have the ability to simultaneously determine two or multi-component PAHs adsorbed onto mangrove leaf surface. Then, in order to overcome the drawback, synchronous SSF and emission fiber-optic fluorimetry (FOF) method were established. [24,25]

Different from the weak autofluorescence signal of leaf surface, mangrove root surface emission relatively strong background fluorescence signal.[26,27] Therefore, the established methods described above can hardly realize *in situ* determination of PAHs adsorbed onto root surface. Recently, highly sensitivity, reliable and accurate laser induced time-resolved nanosecond fluorescence spectroscopy (LITRF) method has been used to reduced the background fluorescence signal and thus realize *in situ* determination single PAHs adsorbed onto mangrove roots.[28] However, we are aware that the excitation, emission and time-resolved fluorescence of many typical PAHs overlap, which limits the standard direct determination of two- or multi-component PAHs by LITRF .

Therefore, in order to simultaneously determination the concentration of mixture fluorescence, as many reports showed, a combination of LITRF and other techniques to separate overlapped fluorescence peak of mixture substance were necessary.[29,30] Among the techniques, chemometrics modeling and derivative fluorometry have been considered to be most efficient. However, when using the chemometrics modelling technique, interference from the scattered light (primarily Rayleigh and Raman scattering) of mangrove roots had a large influence on the estimated model parameters and thus made it difficult to determine the two- or multi-component PAHs adsorbed onto the root surface.[31] Different from the chemometrics modelling technique, fluorescence spectra combined with derivative fluorometry technique was a suitable method to determine the multi-component PAHs in fluorescent substances from complex environmental samples with an interface. [32] Li et al[33] used derivative fluorometry combined with nonlinear variable-angle and matrix-isopotential synchronous scanning mode simultaneously determination multi-component PAHs in tea microwave extraction solvent. Derivative emission fluorescence method was also used to simultaneous analysis of mixture of guaifenesin and phenylephrine in pharmaceutical tables by Macher et al.[34] Both of tea extraction solvent and pharmaceutical table have background fluorescence signal.

In this study, high-sensitivity LITRF and derivative fluorometry techniques were used to establish a novel *in situ* method to determine two-component PAHs (Phenanthrene (Phen) and Fluoranthene (Fla) are two typical and relatively high concentration PAHs in mangrove sediments and plants[35]) adsorbed onto the root surface. This *in situ* method was then used to investigate the transport processes of Phen and Fla adsorbed onto the root surfaces of *Kandelia obovata* (*Ko*), *Bruguiera gymnorhiza* (*Bg*) and *Aegiceras corniculatum* (*Ac*), the three most common mangrove plants along the southeast of China. The effect of temperature, an important environmental factor in regional estuaries, was also considered.

Experimental

Apparatus, reagents and plant

Phen and Fla with a purity of 99.9 % were obtained from Sigma–Aldrich Co. Ltd., UK. All of the other chemicals used in the study were analytical reagents (A.R.) obtained from Sinopharm Chemical Reagent Co. Ltd., China.

A LITRF system purchased from Laser Laboratorium Gottingen GmbH (German) was used to obtain the fluorescence spectra. In this study, the parameters of the LITRF instrument were modified compared with reference[23]: time slice, 180 ns; time width, 5 ns; laser excitation wavelength, 266 nm; emission wavelength, 250-650 nm; channels, 674; exposure time, 125 ms; and cooler temperature, -1℃.

The hypocotyls of *Ko*, *Bg* and *Ac* for cultivation were collected from Yunxiao mangrove swamp (23˚55′ N, 117˚25′ E), a typical mangrove habitat in the Zhangjiang River estuary, Fujian, Southeast China. Mangrove plants were grown in a growth chamber (Safu Co. Ltd., PGX 450B) under a light intensity of 200 μmol m^{-2} s^{-1} with a light cycle of 14/10 h for one year. The temperature (298.15±1 K) and relative water content (70 %) were kept constant.

In all, 5 g of fresh roots were extracted in a Soxhlet extractor using 100 mL of chloroform and methanol (2:1, v/v) mixed solution. The mixed solution was dried and then re-dissolved in 20 mL of hexane. After filtering through filter paper, the solution was dried to a constant weight on a pre-weighed glass. The weight of the residue was calculated as the content of root lipids.[36]

Determination of the PAHs adsorbed onto the root surface of Ko seedlings by LITRF

Several mangrove seedlings of approximately the same height were selected for the experiment. All of these roots were carefully cleaned with distilled water to remove sand, sediment, silt and so on. Special zones with dimensions of 0.5 cm×2 cm (diameter×length) were selected in the taproot to include the divisional and elongation zones. The roots of the mangrove plant were contaminated using the method that we previously reported.[28] Different concentrations of Fla and Phen were slowly and evenly added to mangrove root using 20-μL micropipettes to ensure the homogeneous distribution of the PAHs onto the root surface. After the contamination procedure, the roots were placed onto a specially designed sample holder (the dimension and structure were described in our previous study[28]), and the sensor of the LITRF was fixed on a certain location above the roots. All of the fluorescence spectra were collected by a computer via the software in the LITRF instrument. After deducting a short-lifetime

fluorescence signal (< 10 ns), a program written in Matlab 2014b was used for acquiring the derivative fluorescence spectra.

The transport process of the Phen and Fla from the mangrove root surface to the tissues

Several groups of mangrove seedlings contaminated with the Phen and Fla were used to investigate the PAHs transport processes. Each group had three plants. Both the pre-treatment and determination procedure were the same as in section 2.2. Then, the PAHs-contaminated roots were transferred into amber vials with 5 mL of Mill-Q water (200 mg/L NaN_3) and kept in the dark at temperature (293.15±3 K). The concentrations of Phen and Fla adsorbed onto the root surface were simultaneously determined using the established D-LITRF method at different time intervals to acquire the root uptake kinetics. In addition, the residual concentrations of the PAHs adsorbed onto *Ko*, *Bg* and *Ac* were measured at an equilibrium time of 120 h at different temperature (277.15 , 293.15 , 303.15 , 308.15 and 313.15 K).

Statistical analysis

The three-phase transport model was used to describe the kinetics of the PAHs adsorbed onto the root surfaces and entering the root tissues. The equation of this model was described in reference[28]. The mean and standard deviation values of the replicates for each treatment were calculated, and the data means were compared using one-way analysis of variance (ANOVA) tests. All statistical analyses were run using SPSS version 13.0.

Results and discussion

The optimal condition of the LITRF instrument

A mathematical model for the fibre probe of the LITRF used in this study showed that the main fluorescence signal contribution is due to the limited zones in the solid sample which made the LITRF instrument suitable to determine the PAHs adsorbed onto root surfaces[38]. Then, the optimal conditions for PAHs determination using the LITRF instrument were selected as follows. First, to reduce or overcome the effects of the root dimension on the reproducibility of the fluorescence signal from the PAHs adsorbed onto the root surface, the specially designed sample holder was used, and the relative standard deviation (RSD) obtained in our studies significantly decreased from 11.32 % to 3.11 % for Phen and from 15.22 % to 2.95 % for Fla adsorbed onto a *Ko* root surface. Second, as short-lifetime fluorescence substances were present, the nanosecond time-gated fluorescence method was also used. After determining the short-lifetime fluorescence signal (< 10 ns), as shown in Figure 1b, the auto-fluorescence of the mangrove leaf surface was so low that it would not interfere with the *in situ* determination of the adsorbed PAHs. Third, as the background fluorescence signals of the root surface were almost the same at different distances, the highest intensity of the PAHs fluorescence signal represents the highest signal to noise ratio (S/N). Similar results were observed for *Ac* and *Bg*. Thus, the optimal distances between the optical fibre and the root sample were selected based on the highest S/N of Phen adsorbed onto the root surface, which were 4 mm, 3 mm and 3 mm for *Ko*, *Bg* and *Ac*, respectively. The detailed data are shown in Table S1.

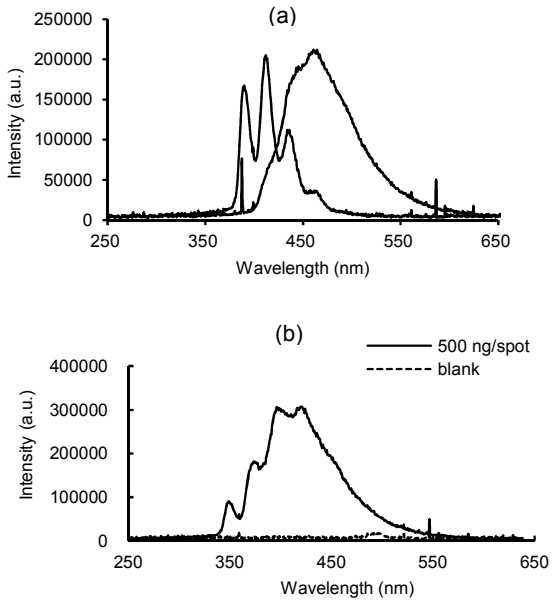

Fig. 1 Fluorescence emission spectra (filter out less than 10 ns fluorescence signals) of the PAHs (Phen and Fla) adsorbed onto root surface of *Ko* seedlings (a) single PAHs (Phen: $\lambda_{em\ max}$=368 nm, Fla: $\lambda_{em\ max}$=428 nm); (b) Phen and Fla

The D-LITRF method for the determination of the Phen and Fla adsorbed onto the surface of mangrove roots

After all of the conditions (sample holder, distance and nanosecond time-gated fluorescence) were adjusted to their optimal values, the fluorescence spectra of Phen and Fla were acquired using the LITRF method. Unfortunately, as shown in figure 1, the emission fluorescence spectra of Phen and Fla adsorbed onto a *Ko* root surface overlapped in the range from 350 to 500 nm which included their maximum emission wavelength (λ_{em}= 368 nm for Phen and λ_{em}= 428 nm for Fla). Therefore, the LITRF method did not have the ability to simultaneously determine the Phen and Fla adsorbed onto a root surface. Moreover, as reports showed[39] that the fluorescence lifetime of Phen and Fla were almost same, it is difficult to simultaneously determine the Phen and Fla adsorbed onto mangrove root surface using only the nanosecond time-resolved fluorescence method.

As previously reports showed, the combination of emission fluorescence spectra with derivative techniques is advantageous in terms of sensitivity and selectivity. Li et al. used this method to simultaneously and rapidly determine benzo[a]pyrene (B[a]P), benzo[k]fluoranthene (B[k]F) and anthracene (Ant) in tea extracts, and the detection limit was as low as 0.11 ng L^{-1} in drinking water.[33,40,41] However, until now, whether the derivative technique combined with LITRF can simultaneously determine Phen and Fla

adsorbed onto a root surface was still largely unknown. Figure 2 shows the fluorescence spectra combined with the first-order derivative technique. It can be clearly seen from this figure that the fluorescence spectra of Phen and Fla adsorbed onto the root surface have been separated after the use of first-order derivative fluorometry. The derivative fluorometry peaks of Phen and Fla were at wavelengths of 345 nm and 391 nm for Phen and Fla, respectively. In addition, the value of the first-order derivative fluorometry of this method increased with increasing concentrations of Phen and Fla adsorbed onto the *Ko* root surface. Similar results were also observed for *Ac* and *Bg*.

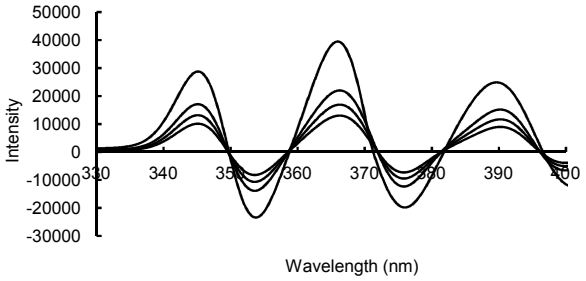

Fig. 2 D-LITRF fluorescence spectra of the Phen and Fla adsorbed onto root surface of *Ko* seedlings. Concentrations of Phen adsorbed from low intensity to high intensity were 60, 100, 150, 300 ng/spot. Concentrations of Fla from low intensity to high intensity were 5, 10, 20, 40 ng/spot.

Analytical merits of the established method

The analytical merits of the method of determination of Phen and Fla were identified. The results are listed in Table 1. The linear ranges were 5.0-700, 4.0-850 and 2.5-1200 ng/spot for Phen adsorbed onto the *Ko*, *Bg* and *Ac* root surfaces, respectively, and 1.0-350, 1.5-550 and 2.0-600 ng/spot for Fla adsorbed onto the *Ko*, *Bg* and *Ac,* respectively. The detection limits were 0.2, 0.2 and 0.1 ng/spot for Phen adsorbed onto the *Ko*, *Bg* and *Ac,* respectively, and 0.1, 0.1 and 0.1 ng/spot for Fla adsorbed onto the *Ko*, *Bg* and *Ac,* respectively. The linear range and detection limits of PAHs using the established method were of the same order as the LITRF method report previously. The results also indicated that the established method acts as a suitable approach for simultaneous *in situ* determination of the Phen and Fla adsorbed onto root surfaces.

Recovery and interference experiment

To confirm the reliability of the D-LITRF method, a recovery experiment was performed. As table 2 showed, the recoveries of the Phen adsorbed onto mangrove plants range from 91.2 % to 106.8 % and the recoveries of the Fla adsorbed onto mangrove plants range from 91.5 % to 115.5 %.

PAHs exist as a mixture and their concentrations vary greatly in the natural environment. Thus, to accurately and simultaneously determine each PAHs adsorbed onto the root surface, it is imperative to make sure that the determination of Phen and Fla did not influence each other. The experimental procedures were the same as those mentioned in reference.[42] The results are listed in table 3. As shown in table 3, when the concentration of Phen was fixed in the middle of its linear dynamic range (400 ng/spot), no influence on the fluorescence signal of Phen was caused by increasing the Fla concentration. A similar conclusion can be drawn from the results for Fla. The results of the analytical merits, and the interference and recovery experiments indicated that the reliability, sensitivity and selectively of this established method meet the requirement of an *in situ* method to investigate the Phen and Fla adsorbed onto root surfaces and entering into root tissues.

Table 1 Analytical merits of the established method (n=9).

Plant	PAHs	Calibration curve	Correlation coefficient	Linear range (ng/spot)	Detection limit[a] (ng/spot)	RSD (%)[b]
Ko	Phen	y[c]=82.76x[d]+4431.6	0.9959	5.0-700	0.23	6.31
	Fla	y=421.25x+6809	0.9936	1.0-350	0.05	7.02
Bg	Phen	y=89.72x+1711.1	0.9966	4.0-850	0.18	5.49
	Fla	y=472.66x+1331	0.9940	1.5-550	0.05	8.32
Ac	Phen	y=151.55x+85.862	0.9997	2.5-1200	0.07	3.49
	Fla	y=800.86x+607.43	0.9963	2.0-600	0.02	4.60

[a] detection limit of the method, which was calculated by $3S_B/m$, where 'S_B' is the standard deviation of the blank, and 'm' is the slope of the calibration curve; [c] RSD represent relative standard deviation [d] y represents the fluorescence intensity of PAHs adsorbed onto the root surfaces of mangrove seedlings; [e] x represents the concentrations of PAHs adsorbed onto the root surfaces of mangrove seedlings.

Transport of Phen and Fla from mangrove root surface to tissues

The reduction of PAHs adsorbed onto root surfaces via dissolution, biodegradation and photodegradation can be neglected in our studies. Therefore, the depuration of PAHs adsorbed onto the root surface was due to the transport of PAHs to root tissues. The presence of lipids was considered to be important for plants to accumulate single PAHs. Li et al. showed that the leaf uptake of Phen was through a channel-like pathway into the middle layer of the cuticle matrix that was composed of a polymeric lipid, and Zhan et al. showed that the content of root lipid was one of the crucial factors for the uptake of PAHs.[43,44] However, the role that lipids played in the transport to root tissues of Phen and Fla adsorbed onto the root surfaces was yet unknown.

Analytical Methods

ARTICLE

Table 2 Results of recovery experiment for the PAHs adsorbed onto the root surfaces (n=9).

PAHs	Plant	Original (ng/spot)	Added (ng/spot)	Total (ng/spot)	Measured (ng/spot)	Recovery (%)	RSD (%)
Phen	*Ko*	50.0	50.0	95.6	45.6	91.2	3.23
		400.0	100.0	511.3	411.3	102.8	4.75
	Bg	50.0	50.0	103.4	53.4	106.8	5.31
		400.0	100.0	505.5	405.5	101.4	2.89
	Ac	50.0	50.0	102.6	52.6	105.2	4.67
		400.0	100.0	490.4	390.4	97.6	6.30
Fla	*Ko*	20.0	50.0	68.3	18.3	91.5	3.28
		200.0	100.0	291.3	191.3	95.7	4.44
	Bg	20.0	50.0	73.1	23.1	115.5	3.36
		200.0	100.0	288.9	188.9	94.5	2.87
	Ac	20.0	50.0	69.0	19.0	95.0	5.01
		200.0	100.0	285.3	185.3	92.7	6.22

Table 3 Results of Interference experiments for Phen and Fla adsorbed onto *Ko*, *Bg* and *Ac* leaves (n=9)

Plant	PAHs		1	2	3	4	5	6
Ko	Phen	Added (ng/spot)	400.0	400.0	400.0	20.0	200.0	400.0
		Found (ng/spot)	397.1	405.3	392.9	18.9	195.7	390.5
	Fla	Added (ng/spot)	20.0	100.0	200.0	200.0	200.0	200.0
		Found (ng/spot)	21.2	98.5	194.6	195.0	202.6	203.1
Bg	Phen	Added (ng/spot)	400.0	400.0	400.0	20.0	200.0	400.0
		Found (ng/spot)	403.3	390.2	394.5	19.6	192.0	398.8
	Fla	Added (ng/spot)	20.0	100.0	200.0	200.0	200.0	200.0
		Found (ng/spot)	19.9	97.3	193.0	205.4	202.5	194.4
Ac	Phen	Added (ng/spot)	400.0	400.0	400.0	20.0	200.0	400.0
		Found (ng/spot)	395.5	391.5	402.6	19.3	191.0	399.5
	Fla	Added (ng/spot)	20.0	100.0	200.0	200.0	200.0	200.0
		Found (ng/spot)	22.7	102.4	203.5	202.1	203.3	196.4

The transport equilibrium coefficient (K_{eq}) is calculated by the equation K_{eq} = (C_0- C_{eq}) /C_{eq}, where C_{eq} (ng/spot) is the concentration of PAHs adsorbed onto the root surface by the time equilibrium was reached and C_0 (ng/spot) is the initial concentration of PAHs adsorbed onto the root surface. The K_{eq} value was 1.20, 1.05 and 1.59 for Phen adsorbed onto *Ko*, *Ac* and *Bg*, respectively, and 1.37, 1.01 and 2.35 for Fla adsorbed onto *Ko*, *Ac* and *Bg*, respectively. Then, the correlations between K_{eq} and the content of root lipids were calculated and the results were displayed in table 4. The linear fitting equations were $y=4.61x_T+2.90$ for Phen and $y=1.85x_T+5.88$ for Fla with the correlation coefficients of 0.9884 for Phen and 0.9862 for Fla being very close to 1. Moreover, the value of K_{eq} showed significant correlation with root lipids ($p< 0.05$).

Moreover, the inhibition rate calculated by the equation: Inhibited rates= (C_s-C_m)/C_s×100 %, where C_s (μg/kg), is the concentration of either Phen or Fla transport to root tissues and C_m (μg/kg) is the concentration of either Phen or Fla transport to tissues in the presence of another PAHs. The inhibited rates, as shown in table 4, of Phen adsorbed onto *Ko*, *Ac* and *Bg* were 27.6 %, 35.4 % and 28.5 %, respectively, and of Fla adsorbed onto *Ko*, *Ac* and *Bg* were 22.7 %, 34.6 % and 21.9 %, respectively. In contrast with the good linear relationship between the content of root lipids and K_{eq}, the inhibit rates showed almost no significant correlation with root lipids ($p> 0.05$). The results indicated that the content of root lipids was an important factor in determining the value of K_{eq} but could not be used to explain the difference in inhibition rates between *Ko*, *Ac* and *Bg*.

Table 4 Correlations between root lipid content and inhibit rates or K_{eq}.

PAHs	Plant	Lipid (mg/g)	K_{eq}	Fitting equation (T [b])	Coefficient (T)	Inhibit rates (%)	Fitting equation (I [c])	Coefficient (I)
Phen	*Ko*	8.59±0.30	1.20	y [d]=4.61x_T [e]+2.90	0.9884	27.6	y=-022x_I [f]+15.42	0.5128
	Ac	7.63±0.15	1.05			35.4		
	Bg	10.19±0.11	1.59			28.5		
Fla	*Ko*	8.59±0.30	1.37	y=1.85x_T+5.88	0.9862	22.7	y=-0.149x_I+12.74	0.6712
	Ac	7.63±0.15	1.01			34.6		
	Bg	10.19±0.11	2.35			21.9		

[a] T represent the fitting equation and correlation coefficients between root lipid and K_{eq}; [b] I represent the fitting equation and correlation coefficients between root lipid and inhibit rates [c] y represents the lipid content of mangrove root; [d] x_T represents the value of K_{eq}; [e] x_I represents the value of inhibit rates.

To further understanding the comparative mechanisms of PAHs transport to root tissues, the transport kinetics for PAHs were also investigated. A three-phase model that was confirmed to be the most suitable model was used to describe PAHs transport to root tissues. Figure 3 shows the three-phase transport model fitting curve for the PAHs, and the fitting parameters (k_{rap}, k_{slow} and $k_{very\ slow}$, Φ and R^2) summarized in table 5. It can be clearly seen from figure 3 and table 5 that with the presence of Fla, the kinetics of the transport of the Phen adsorbed onto root surface to the tissues decreased significantly. There was almost no effect of the co-existing PAHs on the transport to root tissues of the rapid fraction of PAHs adsorbed onto the root surface. The comparative transport of PAHs to root tissues mainly occurred in the slow and very slow stages of PAHs transport. Similar results were obtained with the transport to the root tissues of the Phen and Fla adsorbed onto *Ac* and *Bg* root surfaces. As the slow and very-slow stage was mainly through the active symplastic transport manner of PAHs, the active symplastic movement rather than apoplastic partitioning was responsible for the comparative transport of two-component PAHs to the root tissues.

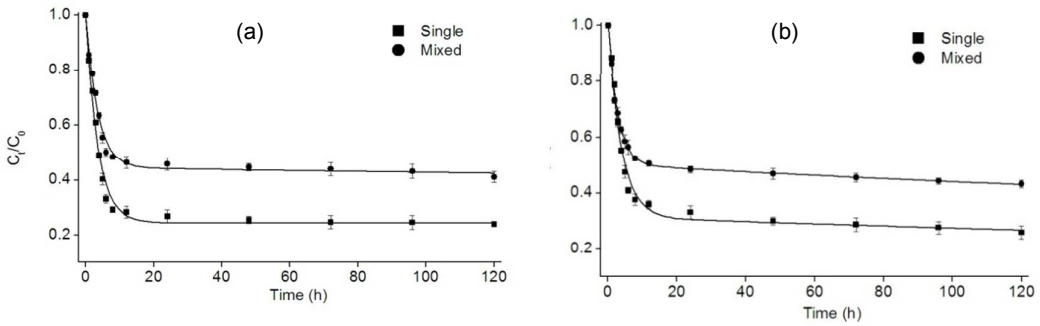

Fig. 3 Transport rate of PAHs (multi-component and single) adsorbed onto root surface to tissues (n=9) (a) Phen; (b) Fla.

Table 5 The kinetic parameters for the transportation of PAHs adsorbed onto *Ko* root surface (n=9)

PAHs	Three-stage model						
	k_{rapid} [c]	k_{slow}	$k_{very\ slow}$	Φ_{rap} [d]	Φ_{slow}	$\Phi_{very\ slow}$	R^2
Phen (S[a])	3.954	0.480	0.025	0.2222	0.4485	0.3293	0.9822
Fla (S)	4.311	0.345	0.003	0.0631	0.2514	0.6855	0.9800
Phen (M[b])	3.883	0.241	0.013	0.1223	0.5451	0.3326	0.9830
Fla (M)	4.280	0.252	0.001	0.0447	0.4511	0.5042	0.9977

[a] S represent the single PAHs adsorbed onto root surface transport to tissues; [b] m represent the multi-component PAHs adsorbed onto root surface transport to tissues. [c] k_{rapid}, k_{slow} and $k_{very\ slow}$ represent the kinetic of rapid, slow and very slow transport , respectively. [d] Φ_{rap}, Φ_{slow} and $\Phi_{very\ slow}$ represent the rapid, slow and very slow transport fraction, respectively.

In addition, as table 4 shows, the transport of Phen to the root tissues was more easily inhibited by the co-existing PAHs. As previously reports showed, the octanol-water partition coefficient (K_{ow}) of PAHs was an important indicator to evaluate whether the PAHs transportation processes were passive apoplastic partitioning or active symplastic movement. The higher the value of K_{ow}, the lower the percentage of PAHs that entered into root tissues through apoplastic movement.[28] The log K_{ow} of Phen was lower than that of Fla, with values of 4.46 and 5.20, respectively (detailed information about physicochemical properties is listed in Table S2). Thus, the percentage of Phen transport to tissues through active symplastic movement is greater than that of Fla and is more easily inhibited by the co-existing PAHs.

Effects of temperature on the transport to tissues of Phen and Fla adsorbed onto Ko root surfaces

Mangrove ecosystems are located on the tropical and subtropical coastal zones. Temperature was one of the important environmental factors that induced plant biological responses and affected the uptake behaviours of many substances.[45] Therefore, the effects of temperature on the transport of two-component PAHs from the surface to the tissues were evaluated.

The effects of temperature on the transport of PAHs from the root surface to the tissues are displayed in figure 4. The transport coefficient for PAHs to tissues (K_{eq}) increased from 0.78 to 1.95 for Phen and from 1.11 to 2.01 for Fla at 277.15-313.15 K, respectively. As a report showed[46], the active symplastic movement of PAHs to the root tissues was an energy-consuming and endothermic process, while the passive apoplastic transport was a non-energy-consuming process. Therefore, the transport of PAHs to root tissues was an energy-consuming, endothermic process, and the K_{eq} of PAHs transport increased with an increase in temperature. Moreover, it can also be clearly concluded from figure 4 that the effects of temperature on the inhibit rates for the transport of PAHs to tissues were clearly divided into two parts. The PAHs transport inhibition rates decreased from 30.4 % to 25.4 % for Phen and from 29.7 % to 20.8 % for Fla with an increasing temperature in the range of 277.15 to 303.15 K. Zhan et al.[47] showed that active symplastic movement was mediated by a PAHs/H^+ symporter system that exists in the plasma membrane. As the temperature increased, the activity of the PAHs symport carrier increased and both Phen and Fla more easily entered into the root tissues through active symplastic movement. Therefore, there was a decrease in the comparative transport of PAHs to root tissues that mainly occurred at slow and very-slow stages and through an active movement manner. However, the PAHs transport inhibition rates increased from 25.4 % to 31.8 % for Phen and from 20.8 % to for 31.2 % Fla at 303.15-313.15 K. The reasons for these results were attributed to the normal physiological status of the plant changing at a high temperature stage and thus significantly decreasing the activity of the PAHs symport carrier.[48]

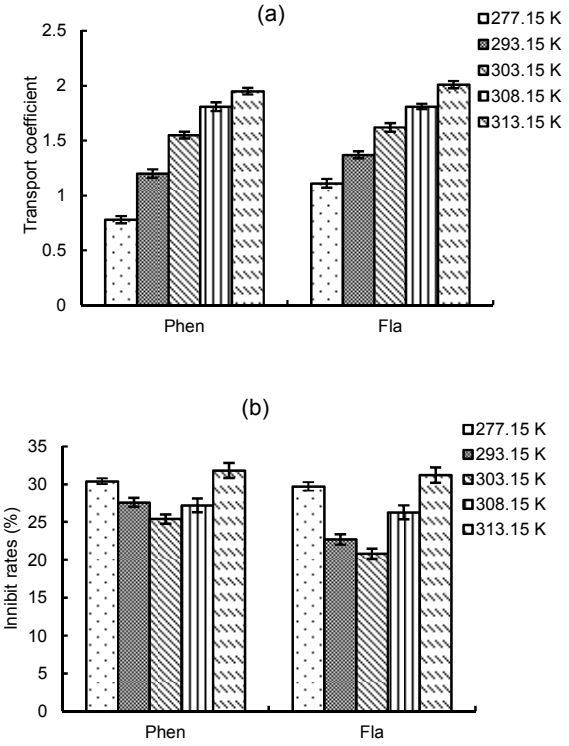

Fig. 4 The inhibit rates and transport coefficient of PAHs adsorbed onto root surface transport to tissues at different temperature (a) inhibit rates; (b) transport coefficient.

Conclusions

The experimental results showed that the combination of the LITRF and first-order derivative fluorometry techniques provide us with a novel approach for the sensitive and accurate *in situ* simultaneous determination of Phen and Fla adsorbed onto root

surfaces. The established method was successfully used to simultaneously investigate the transport of Phen and Fla from mangrove root (*Ko*, *Bg* and *Ac*) surfaces to the tissues. Root lipids played an important role in the transport processes to root tissues of PAHs adsorbed onto the root surfaces. There is a competition in the transportation relationship between Phen and Fla that is due to active symplastic movement. In addition, temperature has the ability to affect the Phen and Fla transport process competition.

However, more studies should be conducted. First, as PAHs in actual environments always exists in a complex composition (16 parent PAHs and other alkylated PAHs), it is necessary to establish a more selective method to simultaneously determine the multi-component PAHs adsorbed onto the root surfaces. Second, with rapid development, there is an increased chance the release of carbon nanomaterial, such as multi-walled or single-walled carbon nanotubes, graphene and so on, into the environment. As this carbon nanomaterial has a strong sorption capacity, it may alter the root uptake, bioaccumulation and bioavailability of PAHs.[49] Therefore, the effects of carbon nanomaterial on the transport of PAHs adsorbed onto root surface also need to be considered.

Acknowledgements

The authors are grateful for financial support from the Natural Science Foundation of China (No. 21177102), the SRFDP (20130121130005).

References

1 J. Z. Wang, C. Z. Zhu, T. H. Chen, PAHs in the Chinese environment: levels, inventory mass, source and toxic potency assessment, *Environ. Sci.: Processes Impacts*, 2013, **15**, 1104-1112.
2 H. Z. Shen, Y. Huang, R. Wang, D. Zhu, W. Li, G. F. Shen, B. Wang, Y. Y. Zhang, Y. C. Chen, Y. Lu, H. Chen, T. C. Li, K. Sun, B. G. Li, W. X. Liu, J. F. Liu, S. Tao, Global atmospheric emissions of polycyclic aromatic hydrocarbons from 1960 to 2008 and future predictions, *Environ. Sci. Technol.*, 2013, **47** 6415-6424.
3 B. Wang, L. Jin, A. Ren, Y. Yuan, J. Liu, Z. Li, L. Zeng, D. Yi, L. L. Wang, Y. Zhang, X. Wang, S. Tao, R. H. Finnell, Levels of polycyclic aromatic hydrocarbons in Maternal serum and risk of neural tube defects in offspring, *Environ. Sci. Technol.*, 2014, **49**, 588-596.
4 B. I. Olu-Owolabi, P. N. Diagboya, K. O. Adebowale, Sorption and desorption of fluorene on five tropical soils from different climes, *Geoderma,* 2015, **239**, 239-240.
5 L. X. Huang, D. X. Gao, Y. Y. Zhang, C. G. Wang, Z. H. Zuo, Exposure to low dose benzo[a]pyrene during early life stages cause symptoms similar to cardiac hypertrophy in adult zeabrafish, *J. Hazard. Mater.* 2014, **276**, 377-382.
6 S. Khan, Q. Cao, Human health risk due to consumption of vegetables contaminated with carcinogenic polycyclic aromatic hydrocarbons, *J. Soil Sediment*, 2012, **12**, 178-184.
7 L. Kacalkova, P. Tlustos, The uptake of persistent organic pollutants by plants, *Cent. Eur. J. Biol.*, 2011, **6**, 223-235.
8 Y. Z. Gao, Y. Zhang, J. Liu, H. L. Kong, Metabolism and subcellular distribution of anthracene in tall fescue (*Festuca arundinacea* Schreb.), *Plant Soil*, 2013, **365**, 171-182.
9 H. X. Lu, Q. Y. Cai, K. C. Jones, Q. Y. Zeng, A. Katsoyiannis, Levels of organic pollutants in vegetables and human exposure through diet, *Crit. Rev. Env. Sci. Tec.*, 2014, **44**, 1-33.
10 M. Waqas, S. Khan, C. Chao, I. Shamshad, Z Qamar, K. Khan, Quantification of PAHs and health risk via ingestion of vegetable in Khyber Pakhtunkhwa Province, Pakistan, *Sci. Total Environ.*, 2014, **497-498**, 448-458.
11 Y. Tian, H. J. Liu, T. L. Zheng, K. K. Kwon, S. J. Kim, C. L. Yan, PAHs contamination and bacterial communities in mangrove surface sediments of the Jiulong River Estuary, China, *Mar. Pollut. Bull.*, 2008, **57**, 707-715.
12 S. Bayen, Occurrence, bioavailability and toxic effects of trace metals and organic contaminants in mangrove ecosystems: A review, *Environ. Int.*, 2012, **48**, 84-101.
13 H. Cheng, Z. Y. Jiang, Y. Liu, Z. H. Ye, M. L. Wu, C. C. Sun, F. L. Sun, J. Fei, Y. S. Wang, Metal (Pb, Zn and Cu) uptake and tolerance by mangroves in relation to root anatomy and lignification/suberization, *Tree Physiol.*, 2014, **34**, 646-656.
14 X. H. Zhan, H. L. Ma, L. X. Zhou, J. R. Liang, T. H. Jiang, G. H. Xu, Accumulation of phenanthrene by roots of intact wheat (*Triticum acstivnm* L.) seedlings: passive or active uptake? *BMC Plant Biol.*, 2010, **10**, 52-59.
15 J. L. Chen, M. H. Wong, Y. S. Wong, N. F. Y. Tam, Modeling sorption and biodegradation of phenanthrene in mangrove sediment slurry, *J. Hazard. Mater.*, 2011, **190**, 409-415.
16 M. J. Riding, K. J. Doick, F. L. Martin, K. C. Jones, K. T. Semple, Chemical measures of bioavailability/bioaccessibility of PAHs in soil: Fundamentals to application, *J. Hazard. Mater.*, 2013, **261**, 687-700.
17 R. C. Hsieh, C. L. Lee, J. F. Jen, K. C. Chang, Complexation-fluocculation combined with microwave assisted headspace solid-phase microextraction in determining the binding constants of hydrophobic organic pollutants to dissolved humic substances, *Analyst*, 2015, **140**, 1275-1280.
18 J. Wang, S. Liu, C. Chen, Y. Zou, H. Hu, Q. Cai, S. Yao, Natural cotton fibers as adsorbent for solid-phase extraction of polycyclic aromatic hydrocarbons in water samples, *Analyst*, 2014, **139**, 3593-3599.
19 L. Bao, P. Sheng, J. Li, S. Wu, Q. Cai, S. Yao, Surface enhanced Raman spectroscopic detection of polycyclic aromatic hydrocarbons (PAHs) using a gold nanoparticles-modified alginate gel network, *Analyst*, 2012, **137**, 4010-4015.
20 Y. Shen, Q. L. Fang, B. L. Chen, Environmental applications of three-dimensional grapheme-based macrostructures: adsorption, transformation, and detection, *Environ. Sci. Technol.*, 2015, **49**, 67-84.
21 P. Wang, K. Z. Du, Y. X. Zhu, Y. Zhang, A novel analytical approach for investigation of anthracene adsorption onto mangrove leaves, *Talanta*, 2008, **76**, 1177-1182.
22 H. F. Sun, R. L. Li, Y. X. Zhu, Y. Zhang, *In situ* determination mechanisms for the depuration of polycyclic aromatic hydrocarbons adsorbed onto leaf surfaces of living mangrove seedlings, *J. Hazard. Mater.*, 2013, **262**, 339-347.
23 H. F. Sun, Y. N. Yang, Y. X. Zhu, Y. Zhang, *In situ* investigation of the depuration of fluoranthene adsorbed on leaf surfaces of living mangrove seedlings, Talanta, 2013, **116**, 441-447.
24 P. Wang, T. H. Wu, Y. Zhang, Direct observation of the photodegradation of anthracene and pyrene adsorbed onto mangrove leaves, *Plos One*, 2014, **9**, e104903.
25 L. Chen, Y. Zhang, B. B. Liu, *In situ* simultaneous determination photolysis of multi-component PAHs adsorbed on the leaf surfaces of living *Kandelia candel* seedlings, *Talanta*, 2010, **83**, 324-331.
26 E. Wild, J. Dent, G. O. Thomas, K. C. Jones, Use of two-photon excitation microscopy and autofluorescence for visualizing the fate and behavior of semivolatile organic chemicals within living vegetation, *Environ. Toxicol. Chem.*, 2007, **26**, 2486-2493.

27 Y. N. Yang, H. F. Sun, Y. X. Zhu, F. Wu, Y. Zhang, *In situ* determination of phenanthrene adsorbed onto surface of mangrove leaves using a laser-induced nanosecond time-resolved fluorescence system, *Chinese J. Anal. Chem.*, 2013, **41**, 1465-1469.
28 R. L. Li, Y. X. Zhu, Y. Zhang, *In situ* investigation of the mechanisms of the transport to tissues of polycyclic aromatic hydrocarbons adsorbed onto the root surfaces of *Kandelia obovata* seedlings, *Environ. Pollut.*, 2015, **201**, 100-106.
29 H. C. Goicoechea, S. Yu, A. F. T. Moore, A. D. Campiglia, Four-way modeling of 4.2 K time-resolved excitation emission fluorescence data for the quantitation of polycyclic aromatic hydrocarbons in soil sample, *Talanta*, 2012, **101**, 330-336.
30 X. D. Zhong, D. S. Fu, P. P. Wu, Q. Liu, G. C. Lin, S. H. Cao, Y. Q. Li, Rapid fluorescence spectroscopic screening method for the sensitive detection of thiabendazole in red wine, *Anal. Methods*, 2014, **6**, 7260-7267.
31 C. M. Andersen, R. Bro, Practical aspects of PARAFAC modeling of fluorescence excitation-emission data, *J. Chemometrics*, 2003, **17**, 200-215.
32 N. Alizadeh, A. Farokhcheh, Simultaneous determination of diphenylamine and nitrosodiphenylamine by photochemically induced fluorescence and synchronous fluorimetry using double scans method, *Talanta*, 2014, **121**, 239-246.
33 X. Y. Li, N. Li, H. D. Luo, L. R. Lin, Z. X. Zou, Y. Z. Jia, Y. Q. Li, A novel synchronous fluorescence spectroscopic approach for the rapid determination of three polycyclic aromatic hydrocarbons in tea with simple microwave-assisted pretreatment of sample, *J. Agric. Food Chem.*, 2011, 59, 5899-5905.
34 H. M. Maher, M. M. Alshehri, S. M. Al-taweel, Derivative emission spectrofluorimetry for the simultaneous determination of guaifenesin and phenylphrine hydrochloride in pharmaceutical tablets, *Luminescence*, 2015, 30, 330-336.
35 F. Li, X. Zeng, J. Yang, K. Zhou, Q. Zan, A. Lei, N. F. Y. Tam, Contamination of polycyclic aromatic hydrocarbons (PAHs) in surface sediments and plants of mangrove swamps in Shenzhen, China, *Mar. Pollut. Bull.*, 2014, **85**, 590-596.
36 H. Li, G. Y. Sheng, C. T. Chiou, Q. Y. Xu, Relation of organic contaminant equilibrium sorption and kinetic uptake in plants, *Environ. Sci. Technol.*, 2005, **39**, 4864-4870.
37 A. H. Rhodes, L. E. McAllister, K. T. Semple, Linking desorption kinetics to phenanthrene biodegradation in soil, *Environ. Pollut.*, 2010, **158**, 1348-1353.
38 U. Bunting, P. Karlitschek, Mathematical model for optimum fiber optics probe design and characterization, *Spectrochim Acta A*, 1998, **54**, 1369-1374.
39 E. Selli, C. Zaccaria, F. Sena, G. Tomasi, G. Bidoglio, Application of multi-way models to the time-resolved fluorescence of polycyclic aromatic hydrocarbons mixture in water, *Water Res.*, 2004, **38**, 2269-2276.
40 N. Zhou, H. D. Luo, N. Li, Y. Z. Jia, Highly sensitivity and selective spectrofluorimetric approach for the rapid determination of trace benzo[a]pyrene in drinking water and in solutions leached from disposable paper cups, *Luminescence*, 2011, **26**, 35-43.
41 A . Andrade-Eiroa, G. De-Armas, J. M. Estela, V. Cerda, Critical approach to synchronous spectrofluorimetry, *TRAC-Trend Anal. Chem.*, 2010, **29**, 885-901.
42 L. Z. Sang, X. Y. Wei, J. N. Chen, Y. X. Zhu, Y. Zhang, Simultaneous fluorimetric determination of the biodegradation processes of dissolved multi-component PAHs, *Talanta*, 2009, **78**, 1339-1344.
43 Q. Q. Li, B. L. Chen, Organic pollutant clustered in the plant cuticular membranes: Visualizing the distribution of phenanthrene in leaf cuticle using two-photon confocal scanning laser microscopy, *Environ. Sci. Technol.*, 2014, **48**, 4774-4781.
44 X. H. Zhan, X. Liang, G. H. Xu, L. X. Zhou, Influence of plant root morphology and tissue composition on phenanthrene uptake: Stepwise multiple linear regression analysis, *Environ. Pollut.*, 2013, **179**, 294-300.
45 S. A. Boczulak, B. J. Hawkins, R. Roy, Temperature effects on nitrogen form uptake by seedlings roots of the three contrasting conifers, *Tree Physiol.*, 2014, **34**, 513-523.
46 X. H. Zhan, X. Liang, T. H. Jiang, G. H. Xu, Interaction of phenanthrene and potassium uptake by wheat roots: a mechanistic model, *BMC Plant Biol.*, 2013, **13**, 168-176.
47 X. H. Zhan, X. B. Zhang, X. M. Yin, H. L. Ma, J. R. Liang, L. X. Zhou, T. H. Jiang, G. H. Xu, H^+/phenanthrene symporter and aquaglyceroporin are implicated in phenanthrene uptake by Wheat (*Triticum aestivum* L.) roots, *J. Environ. Qual.*, 2012, **41**, 188-196.
48 A. S. Mathieu, S. Lutts, B. Vandoorne, C. Descamps, C. Perilleux, V. Dielen, J. C. Van Herck, M. Quinet, High temperatures limit plant growth but hasten flowering in root chicory (*Cichorium intybus*) independently of vernalisation, *J. Plant Physiol.*, 2014, **171**, 109-118.
49 J. Zhao, Z. Y. Wang, J. C. White, B. S. Xing, Graphene in the aquatic environment: adsorption, dispersion, toxicity and transformation, *Environ. Sci. Technol.*, 2014, **48**, 9995-10009.